Rapid Mode Decomposition of Few-Mode Fiber By Artificial Neural Network

Han Gao, Zhuo Chen, Yan-Xin Zhang, Wei-Gang Zhang, Hai-Feng Hu, and Tie-Yi Yan

***Abstract*—A novel method based on deep learning technique for the modal decomposition of the optical fields emerging from the few-mode fiber is demonstrated in this paper. By combining the advantages of principal component analysis (PCA) and Back-Propagation (BP) neural network, this scheme can reveal the exact superposition of eigenmodes. Firstly, PCA algorithm is applied to preprocess the target samples to reduce the computational complexity and extract the characteristics of the samples. Then, the mapping between the mode coefficients and the preprocessed near-field beam patterns is learned by using the BP neural network. The superiority of the proposed scheme is evaluated through simulation and experiment. The results show that the scheme can perform a complete modal decomposition within a few milliseconds, and it can still work well when the SNR level is as low as 20 dB. It is also worth noting that the method described in this work also has the advantages of short network training time, non-iterative, and low experimental equipment requirements.**

***Index Terms*—Deep learning, fiber characterization, modal decomposition, optical fiber.**

I. Introduction

MODAL decomposition (MD) technology depicts an essential measurement tool and provides the modal characteristics in the light emitting from fiber. Within that context, MD techniques are frequently adopted to study fiber bending [1], fiber coupling process [2], as well as to measurement the beam quality [3] and realize adaptive mode control [4]. Specifically, MD techniques can be divided into two categories. One is the experimental-based MD technology, which can directly obtain modal characteristics through experiments, such as spatially and spectrally resolved imaging (S2) method [5], cross-correlated imaging in the frequency domain (fC2) method [6], three-mirror ring resonator method [7], and computer-generated hologram (CGH) method [8], etc. There is no doubt that all of the above-mentioned technologies have demonstrated outstanding merits. However, these schemes have particularly high requirements in terms of experimental realization, temporal effort and necessary equipment. In contrast to above methods, the numerical MD technique based on the measured optical intensity distribution stands out due to its significantly low experimental workload, such as stochastic parallel gradient descent algorithm [9]–[11], Gerchberg-Saxton algorithm [12], and simplex-search algorithm [13], etc. Note that these algorithms may fall into local minimums due to the sensitivity of the initial value. The hybrid algorithm constructed by combining the advantages of the local search algorithm and the global optimization algorithm is an effective method to solve this problem, but the convergence time will also increase significantly [14]. Some non-iterative numerical demodulation methods, such as matrix inversion method [15] and fractional Fourier system [16], can avoid the above problems and have demonstrated excellent performance.

As a research hotspot in recent years, deep learning (DL) has made outstanding achievements in many fields [17], [18]. Recently, DL has also had successful applications in optics and photonics [19]–[21]. Inspired by these successful applications, some researchers have tried to verify whether similar successes can be replicated in the field of mode demodulation, and breakthroughs have been made [22]–[26]. Some researchers have successfully applied convolutional neural networks to perform MD, and the demodulation rate can reach about 30 Hz [23], [25]. Notwithstanding this notable progress, the decomposition methods based on DL still have some problems that cannot be ignored. For example, this method takes a long time to train the model and requires a high-performance computer. In the 3-mode case, it still takes 8 hours to train the network even when GPU acceleration technology is used [23], [25].

In this work, we examined a novel method based on artificial neural networks to reveal the precise superposition of eigenmodes in few-mode fiber, which combines the advantages of principal component analysis (PCA) algorithm and Back-Propagation (BP) neural network. Firstly, the PCA algorithm is used to remove redundant information and noise in the samples, which will reduce the complexity of subsequent calculations and increase the convergence speed. Then, the target samples after dimensionality reduction will be utilized to train the BP neural network to achieve the purpose of learning the mapping between the model coefficients and the near-field beam patterns. Experimental and simulation results show the superiority of the scheme. In the 3-mode case, it takes ∼1 hour to train the model, and ∼40 milliseconds to perform a complete MD. After optimizing the data set, the demodulation time is reduced to

Manuscript received April 12, 2021; revised May 28, 2021, June 25, 2021, and July 9, 2021; accepted July 12, 2021. Date of publication July 16, 2021; date of current version October 4, 2021. This work was supported in part by the National Natural Science Foundation of China under Grants 11874226 and 62075132. *(Corresponding authors: Wei-Gang Zhang, Hai-Feng Hu.)*

Han Gao, Yan-Xin Zhang, Wei-Gang Zhang, and Tie-Yi Yan are with the Institute of Modern Optics, Nankai University, Tianjin 300350, China (e-mail: 1120200117@mail.nankai.edu.cn; 1120190104@mail.nankai.edu; zhangwg@nankai.edu; yanty@nankai.edu.cn).

Zhuo Chen and Hai-Feng Hu are with the School of Optical-Electrical and Computer Engineering, University of Shanghai for Science and Technology, Shanghai 200093, China (e-mail: 202310328@st.usst.edu.cn; hfhu@usst.edu.cn).

Color versions of one or more figures in this article are available at https://doi.org/10.1109/JLT.2021.3097501.

Digital Object Identifier 10.1109/JLT.2021.3097501

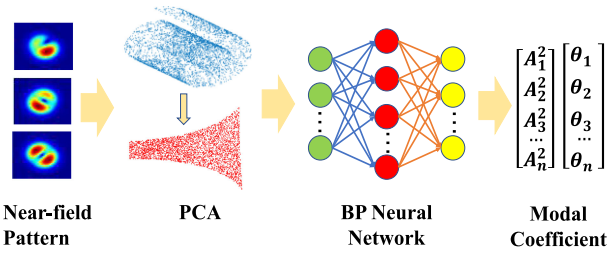

Fig. 1. The principle of modal demodulation scheme based on artificial neural network.

~5 milliseconds. It is worth noting that the scheme proposed in this paper can still work well when the SNR level is as low as 20 dB. In addition, compared with the previously proposed DL-based modal demodulation method, the scheme described in this work significantly reduces the time spent on training models and does not require GPU acceleration technology, which undoubtedly further expands the application scope of this scheme. We believe that the work described here will be a cornerstone for the study concerning the optical fiber numerical MD based on DL.

II. Principle of Operation

A. Principle of the Scheme

The propagating field within the fiber can be expanded as [15]:

$$U(r) = \sum_{n=1}^{n_{\max}} A_n e^{(i\theta_n)} \psi_n(r) \tag{1}$$

where $\psi_n(r)$ is the field distribution of the *n-th* eigenmode, ${A_n}^2$ is the modal weight and θ_n is the modal phase. MD depicts an elegant measurement tool and provides ${A_n}^2$ and θ_n from the near-field pattern. We define an evaluation function $f(k)$ to quantify the correlation between predicted and true values [15]:

$$f(k) = \frac{\sum_{x,y} (I_0(x,y) - \bar{I}_0)(I_k(x,y) - \bar{I}_k)}{\sqrt{\sum_{x,y} (I_0(x,y) - \bar{I}_0)^2 \sum_{x,y} (I_k(x,y) - \bar{I}_k)^2}} \tag{2}$$

where I_0 is the target intensity distribution, I_k is the reconstructed intensity distribution, $\bar{I}_0$ and $\bar{I}_k$ are the average values of I_0 and I_k, respectively. A larger $f(k)$ indicates higher correlation between the reconstruction intensity distribution and the target intensity distribution.

The scheme described in this work is shown in Fig. 1. Firstly, the near-field intensity patterns emerging from the few-mode fiber are stored as training samples. Then, the training samples processed by the PCA algorithm for dimensionality reduction are fed into the BP neural network to train a model that can directly predict the model coefficients. PCA is one of the most commonly used data dimension reduction methods, and has been widely used in various fields [27]. It follows the principle of representing the characteristics of the original data as much as possible, and projects the data in the original space into a low-dimensional coordinate system. Generally speaking, due to the removal of noise and redundant information, there is a more accurate mapping relationship in the new coordinate system. BP neural network is a multi-layer feedforward network, and it is one of the most widely used neural networks [28]. The core idea of the BP network is to propagate the output error to the input layer through the hidden layer in some form and continuously modify the connection weights until the error of the network output is reduced to an acceptable level.

In this experiment, the near-field intensity pattern after dimensionality reduction by the PCA algorithm is integrated into a vector, which will be used as the input of the BP neural network. The modal weight or modal phase is also reconstructed into a vector, which will be utilized as the label vector of the input vector to train the BP neural network. It is worth noting that the modal phase used in training is the relative phase difference between the higher-order mode and the fundamental mode. Moreover, there may be phase ambiguity in the experiment. The reason is that only the near-field intensity mode is used in the numerical mode decomposition, so the real field and the conjugate field cannot be distinguished [29]. Therefore, the real phase cannot be used directly when generating the label vector, which will confuse the BP neural network and reduce the accuracy of the network. To solve this problem, the cosine value will be used to replace the real phase to ensure the consistency of the training data [23].

The value of the modal weight can be directly obtained when the trained BP neural network is used to predict the mode coefficients. However, for the modal phase, it is necessary to calculate all possible combinations based on the predicted cosine value, and Eq. 2 will be employed to determine the most likely phase combination. Eq. 2 represents the similarity between the target intensity distribution and the reconstructed intensity distribution, and the closer its value is to 1, the higher the similarity is. Furthermore, the training data must be normalized.

The samples used to train the model here are obtained through simulation, and then the trained model is tested by simulation data and experimental data respectively. By randomly generating the modal weights in the range of 0 to 1 and the modal phases in the range of -π to π, the near-field intensity image used for training the model can be obtained. Specifically, if the number of eigenmodes supported in the optical fiber is *N*, then the *N* amplitudes $\{A_1\ A_2\ \ldots A_N\}$ and *N-1* phase differences $\{\theta_1\ \theta_2\ \ldots \theta_{N-1}\}$ are encoded into a *2N-1* dimensional label vector. By substituting the label vector into Eq. 1, the corresponding near-field beam intensity image can be obtained.

The experiments described in this paper are all carried out on a laptop with an Intel Core i5-7300 CPU. When the PCA algorithm is utilized to perform data dimensionality reduction, 10000 randomly generated images with a resolution of 250∗250 are used to construct a low-dimensional space. A reasonable choice of the dimensions of a low-dimensional space is crucial. In practical applications, the eigenvalues of the covariance matrix of the samples are usually used to describe the amount of information contained in the direction of the corresponding eigenvector. Therefore, the dimension can be determined according to the amount of information that needs to be retained. In this work, we reduced the dimension of the samples from 62500 (250∗250) to 50.

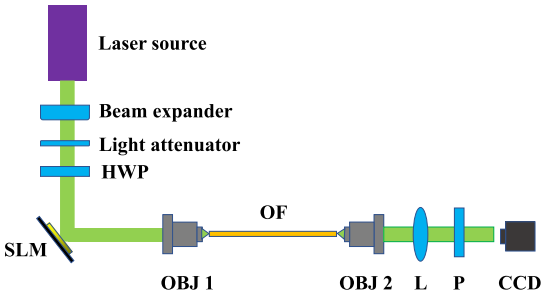

Fig. 2. The experimental setup for recording the mode field of 3-mode optical fiber. HWP, half-wave plate; P, linear polarizer; OBJ, microscope objective lens; L, lens; OF, 3-mode fiber; CCD, Charge Coupled Device camera.

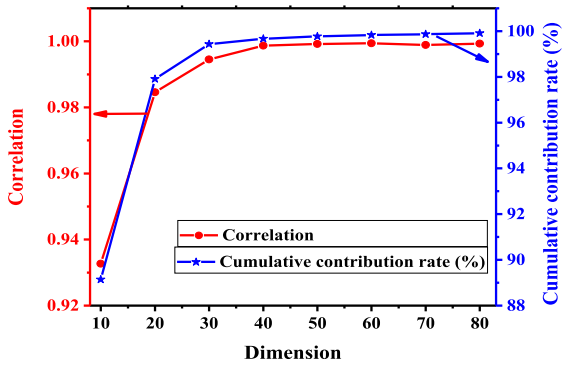

Fig. 3. Average correlation and cumulative contribution rate under different dimensions.

In the subsequent work, 50000 images with a resolution of 250∗250 were randomly generated as the data set, and the data set after dimension reduction was used to train BP neural network. To prevent overfitting, the validation check is used as the termination condition in this work, and the number of validation checks is set as 6 times. Taking the validation check as a termination condition means that during the training process, if the error curve of the validation set samples no longer drops for 6 consecutive iterations, then the calculation will be stopped. Therefore, the number of iterations of BP neural networks designed for different targets is different.

During the experiment, we found that even if the structure of the neural network is relatively simple, the modal weights with high accuracy can be obtained. However, it is necessary to design a more complex network to obtain the modal phases with similar accuracy. Therefore, if only one BP neural network is used to predict the modal weight and modal phase simultaneously, then it must have a complex network structure, which will greatly increase the computational complexity and convergence time. To solve this problem, we trained prediction models for modal phase and modal weight respectively.

B. Experimental Setup

The experimental setup used to record the mode field at the output end of the optical fiber is shown in Fig. 2.

The light emitted from the light source (1550 nm, Santec TSL-550) is first transmitted to the spatial light modulator (SLM) after pre-processing, and is modulated by SLM. Then, the modulated light is coupled into the 3-mode optical fiber (OF, YOFC FM2010) using the microscope objective lens 1 (OBJ 1) for transmission, and the length of the 3-mode optical fiber is 1m. Finally, the light beam emitted from the distal end of the optical fiber is recorded by the charge coupled device (CCD) camera after passing through the 4*f* imaging system composed of OBJ 2 and lens (L). SLM can flexibly and rapidly change the phase distribution of the incident beam, so it is convenient to obtain a variety of mode field distributions at the output end of the fiber by manipulating SLM. In this work, a total of 300 samples with different modal field distributions were collected. These samples will be sorted into a test set and sent to the trained model for real-time MD to test the generalization ability of the proposed scheme. It should be noted that no radiation modes are observed at the output end of the fiber. Because the coating layer is not removed in this work, the cladding modes (radiation modes) are largely attenuated in the propagation process.

III. Results and Discussion

A. Simulation Results and Discussion

Take the 3-mode case as an example, we trained two BP neural networks and randomly generated 1000 near-field intensity patterns for testing. In this experiment, ΔP and $\Delta\theta$ defined in Eq. 3 and Eq. 4 are used to numerically describe the modal weight error and modal phase error between the reconstructed intensity distribution and the target intensity distribution. Subsequently, the comparison between the reconstructed intensity distribution image and the target intensity distribution image will be shown to intuitively evaluate our method.

$$\Delta P = \left|{A_1}^2 - {A_2}^2\right| \tag{3}$$

$$\Delta\theta = \left||\theta_1| - |\theta_2|\right| \tag{4}$$

where ${A_1}^2$ and θ_1 are the real values, ${A_2}^2$ and θ_2 are the predicted values.

Taking the 3-mode case as an example, a set of comparative experiments was conducted to study the relationship between the dimensionality of the low-dimensional space and the demodulation accuracy. In order to more directly describe the number of features contained in the low-dimensional space, the cumulative contribution rate is used to express the ratio of the features contained in the low-dimensional space to the total features. The results of the comparative experiment are shown in Fig. 3. It can be found that the cumulative contribution rate and the averaged correlation increase with the increase of the low-dimensional space dimension. When the dimensionality of the low-dimensional space reaches 50, the correlation is 0.9992. However, the calculation accuracy has some small fluctuations with the further increase of the dimensionality of the low-dimensional space. This shows that when the dimensionality of the low-dimensional space increases to a certain extent, some of the introduced features may not be useful, and it also shows that the calculation accuracy is not directly proportional to the dimensionality of the low-dimensional space. Therefore, after thorough consideration, the dimension of the low-dimensional space selected in this work is 50.

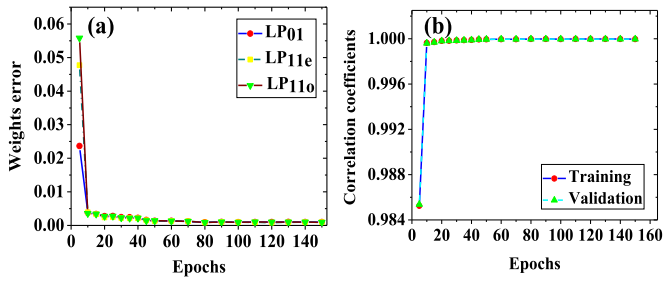

Fig. 4. The training process of modal weights as a function of epochs. (a) modal weights error of different modes (b) correlation coefficients between the target value and the predicted value.

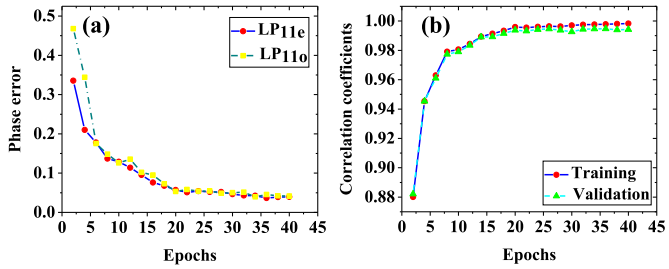

Fig. 5. The training process of modal phase as a function of epochs. (a) modal phase error of different modes (b) correlation coefficients between the target value and the predicted value.

The structure of the BP neural network used to predict the modal weight is 50-30-14-3. This network has 3 layers, in which the input layer has 50 neurons, the hidden layer 1 has 30 neurons, the hidden layer 2 has 14 neurons, and the output layer has 3 neurons. Fig. 4(a) describes the relationship between epochs and the weight errors of different modes, and Fig. 4(b) shows the correlation between the target value and the predicted value. It should be noted that the modal weight error and phase error described in this experiment are the mean values of 1000 samples. It can be noticed that the BP neural network can quickly converge to a relatively good level after 10 training epochs, and stop training after 150 training epochs. The correlation coefficient R value is used to express the correlation between the target value and the predicted value. The closer the correlation coefficient is to 1, the higher the accuracy of the prediction. After 10 training epochs, the average modal weight error of the three modes is 3.76E-3, and the correlation coefficients between the real value and the predicted value on the training set and the verification set were 0.99963 and 0.99960, respectively. When the training is terminated, the average modal weight error of the three modes is 9.55E-4, and the correlation coefficients of the training set and the validation set are 0.99997 and 0.99997, respectively.

The structure of the BP neural network used to predict the modal phase is 50-30-30-30-2. This network has 4 layers, in which the input layer has 50 neurons, the hidden layer 1 has 30 neurons, the hidden layer 2 has 30 neurons, the hidden layer 3 has 30 neurons, and the output layer has 2 neurons. Fig. 5(a) describes the relationship between the phase errors of different modes and epochs, and Fig. 5(b) shows the changes in the learning curve of the BP neural network. It can be noticed that the BP neural network can quickly converge to a relatively good level after 20 training epochs, and stop training after 40 training epochs.

TABLE I
CONSUMING TIME FOR THE BP NEURAL NETWORK

	T_1	T_2	T_3	T_4
modal phase	4.01 s	37 min	0.33 s	38.37 s
modal weight	/	24 min	0.42 s	/

TABLE II
AVERAGED ERROR OF MODAL WEIGHTS AND MODAL PHASE

	LP_{01}	LP_{11e}	LP_{11o}	Average
modal weight	9.94E-4	9.48E-4	9.23E-4	9.55E-4
modal phase	/	3.95E-2	4.14E-2	4.05E-2

The details of modal weight error, modal phase error and the time spent are summarized in Table I and Table II, respectively. In Table I, T_1 represents the time for image preprocessing, T_2 represents the time for training the BP neural network, T_3 represents the time for prediction with the trained BP neural network, and T_4 represents the time for selecting the most suitable phase combination. Image preprocessing only needs to be done once. It can be found from Table I that it takes 43.13 s to complete the MD of 1000 samples by using the trained BP neural network, among which the image preprocessing requires 4.01 s, the phase calculation requires 38.7 s, and the modal weight calculation requires 0.42 s. Note that each sample only takes 43.13 milliseconds to perform MD. The speed of the numerical modal demodulation method based on iterative algorithm can reach 113 milliseconds per frame [11]. Compared with the demodulation scheme based on iterative algorithm, the scheme proposed in this paper has advantages in speed. At present, among the reported numerical modal demodulation methods, only the matrix inversion method has a faster demodulation speed than the scheme based on machine learning, and the speed of the matrix inversion method can reach about 10 μs per frame [15].

Table II shows the average modal weight error and average modal phase error of 1000 test samples in the 3-mode case. It can be found that the modal weight error and the modal phase error have reached the order of 1E-4 and 1E-2 respectively. At this time, the average value of the evaluation function of 1000 samples is 0.9992. Compared with the reported efforts [15], [23], [25], the scheme proposed in this paper can achieve similar demodulation accuracy. It can be concluded that the trained BP neural network can learn the relationship between the mode coefficient and the near-field beam intensity images. In addition, if only the modal weights need to be extracted, the running time will be reduced to ~4 milliseconds. Therefore, the method proposed in this work has a broad application space in some application areas where only accurate modal weights are required [30]–[33].

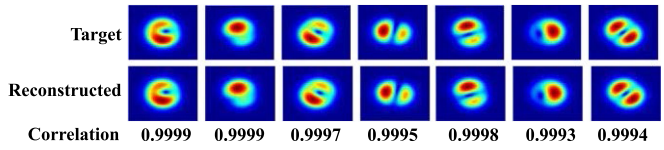

Fig. 6. Numerical MD of 3-mode case based on BP neural network.

In order to evaluate the scheme visually and intuitively, the reconstructed intensity patterns and target intensity patterns of several sets of samples are collected in Fig. 6. In addition, the correlation is also described in Fig. 6. It can be found that the reconstruction intensity patterns and the target intensity patterns are highly similar, which further confirms the accuracy and effectiveness of the method described in this work.

The performance of BP neural network may be improved by increasing the number of samples included in the training set. After increasing the number of training samples from 50000 to 150000, the average modal weight error and modal phase error decrease from 9.55E-4 and 4.05E-2 to 5.41E-4 and 3.58E-2, respectively, and the averaged correlation increased from 0.9992 to 0.9993. However, the training time is getting longer with the increase of training samples. The training time of modal weight and phase is increased from 34 min and 26 min to 285 min and 237 min, respectively. In addition, the prediction accuracy of the BP neural network can be improved by increasing the complexity of the network structure, optimizing the initial value of the network with the algorithm, and constructing the hybrid algorithm.

It can be found from Table I that the main reason that affects the demodulation speed is that it takes a long time to select the most suitable phase combination. This is because the cosine of the phase is used as the label vector in order to avoid the influence of the conjugate field. The data set can be optimized to solve this problem. In the new data set, the range of θ_2 is 0 to π, and the range of $\theta_{3,4,5\ldots N}$ is 0 to 2π. In this case, the label vector is composed of the phase itself, which can not only avoid the loss of phase information, but also improve the demodulation speed. The results show that in the 3-mode case, the average correlation of the test samples when using the new data set is 0.9993, and it takes about 5 milliseconds to perform a complete modal demodulation.

In order to test the generalization ability of the proposed scheme, we also train the network for 5-mode, 6-mode, 8-mode and 10-mode cases. As the number of modes increases, the combination of eigenmodes becomes more complex, and the number of similar near-field beam patterns with different mode coefficients also increases. Therefore, in order to ensure the accuracy of demodulation, it is necessary to increase the learning ability of the BP network. In this work, we optimize the network by increasing the number of hidden layers and the number of neurons in the BP network to achieve the purpose of increasing the learning ability. In addition, in order to describe the solution space more comprehensively, it is also necessary to increase the number of images in the training set and the dimensionality of the input data of the BP neural network. In this work, the architectures of the amplitude prediction network used in the 5-mode case, the 6-mode case, the 8-mode case, and the 10-mode case are 60-30-15-5, 60-30-18-6, 70-30-20-8 and 90-30-25-10, respectively, and the phase prediction network architectures used are 60-45-45-45-4, 60-50-50-50-5, 70-50-40-40-40-7 and 90-60-60-60-60-9, respectively. The number of pictures in the training set used in these cases are 100000, 200000, 300000 and 400000 respectively. Fig. 7 describes the relationship between the number of modes and correlation. It can be found that the correlation decreases as the number of supported modes increases. The matrix inversion method can demodulate up to 27 modes [15], but the demodulation scheme based on DL does not show comparable generalization capabilities when supporting more modes. The reason may be that the expansion of modes will lead to an increase in the number of similar near-field beam patterns with different mode coefficients, which will introduce ambiguity [23]. One promising way to reduce this error is to introduce far-field beam intensity image. The far-field beam patterns corresponding to similar near-field beam patterns with different mode coefficients are completely different. Therefore, by combining the near-field beam pattern and the far-field beam pattern, the BP network is promising to accurately predict the mode coefficient with almost no ambiguity. It can be found from Fig. 7 that when the number of modes to be studied is less than or equal to 5, the proposed scheme is robust to perform accurate MD. Otherwise, the proposed scheme needs to be optimized according to the above discussion.

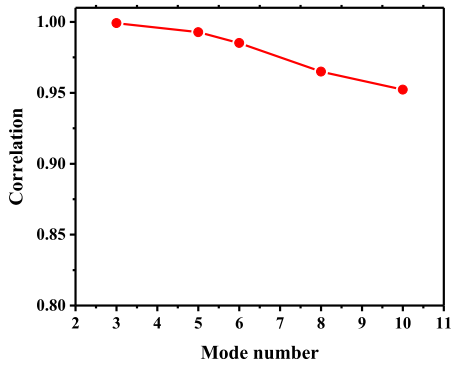

Fig. 7. The relationship between the mode number and the correlation.

The robustness of the BP neural network is verified by adding Gaussian noise to the ideal clean sample. Gaussian noise refers to a type of noise whose probability density function obeys Gaussian distribution, which is very commonly used in theoretical research. Similarly, we randomly generate 1000 samples, and feed the samples under different noise intensities to the trained BP neural network to obtain the predicted mode coefficients. Fig. 8 depicts the performance of the BP neural network for noisy input samples. It can be found that the DL-based scheme proposed in this paper can still work well when the SNR level is as low as 20 dB in our numerical example. To evaluate the noise sustainability of the proposed scheme, we use the following metrics [15]:

$$E_{NET} = \frac{\|C^{true} - C^{recover}\|}{\|C^{true}\|} \tag{5}$$

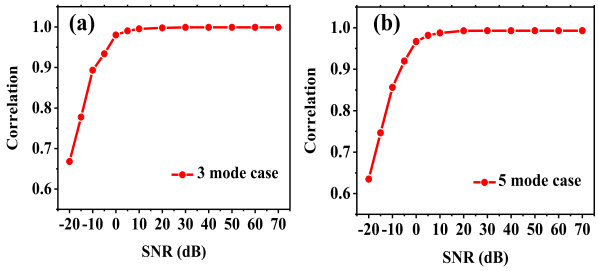

Fig. 8. The performance of BP neural network for noisy input samples. (a) 3-mode case (b) 5-mode case.

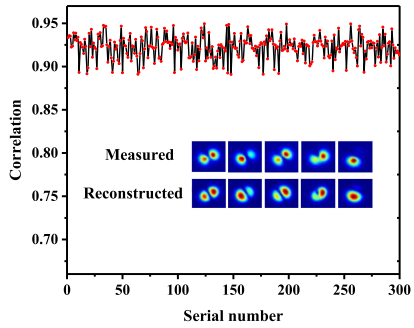

Fig. 9. Experimental results of performing modal demodulation on a 3-mode fiber. The inserted pictures are several representative measured and reconstructed intensity images.

where E_{NET} is the total error and $C = A\exp(i\theta)$ is the complex coefficient. The simulation results show that the scheme proposed in this paper can be applicable for MD with a total error of 0.1 at a SNR level of 1 dB for 3-mode case and at a SNR level of 5 dB for 5-mode case correspondingly. For the 6-mode case and the 8-mode case, the corresponding SNR levels are 10 dB and 20 dB, respectively. In the previously reported non-DL demodulation scheme, the SNR level is limited to 20 dB [15], [16]. The SNR level of the matrix inversion method is limited to 20 dB for the 3-mode case and 30 dB for the 5-mode case [15]. The SNR level of the fractional Fourier system for the 6-mode case is limited to 20 dB [16]. In comparison, the scheme proposed in this paper has better noise sustainability. The main reason is that the data-driven DL model has better anti-interference ability. In addition, adding noise to the training set can further improve the anti-noise ability of the network.

In order to describe the superiority of the proposed scheme more clearly, it is necessary to quantitatively evaluate the performance of the framework. Firstly, the scheme proposed in this paper is compared with the previous demodulation scheme based on DL [23], [25]. The scheme proposed in this paper and the demodulation scheme based on CNN architecture have similar demodulation accuracy and generalization ability [23], [25]. In terms of model training time, the scheme proposed in this paper takes about 1 hour to train a model for 3-mode cases, while the demodulation scheme based on CNN takes 8 hours. In contrast, the scheme proposed in this paper has advantages in training time. In terms of demodulation speed, the CNN-based demodulation scheme requires about 8 to 10 milliseconds to perform a complete modal demodulation, while the method proposed in this paper requires about 40 milliseconds. After optimizing the label vector of the data set, the demodulation time of the proposed scheme is reduced to about 5 milliseconds. In terms of hardware requirements, the experiments described in this paper are all carried out on a laptop with an Intel Core i5-7300 CPU, and the CNN-based demodulation schemes are all carried out on a desktop computer with an Intel Core i7-8700 CPU and GTX 1080 GPU. It can be found that the demodulation scheme proposed in this paper has lower hardware requirements than the CNN-based demodulation scheme. Next, the scheme proposed in this paper is compared with the reported non-DL demodulation scheme. From the previous discussion, it can be found that the scheme proposed in this work has advantages in terms of anti-noise capability and demodulation speed. However, due to its data-driven characteristics, the generalization ability of the scheme proposed in this paper needs to be improved. Some promising ways to further improve the learning and generalization capabilities of the model include designing more complex networks, using more training data, and increasing the resolution of training samples.

B. *Experimental Results and Discussion*

The experimental setup described in Fig. 2 for recording the 3-mode fiber mode field was used to collect test images. The PCA algorithm will reduce the dimensionality of the experimental data after preprocessing. Then, the reduced data is fed into the trained BP neural network model one by one for modal demodulation.

A total of 300 images were recorded in this experiment, and the demodulation results are shown in Fig. 9. The averaged correlation between reconstructed images and target images of 300 test samples is 0.9224, and representative target images and the corresponding reconstructed images are inserted into Fig. 9. It can be concluded from Fig. 9 that the similarity between the reconstructed image and the test image is high, showing the accuracy of our scheme.

It is also worth noting that the mean correlation of the test samples in the simulation is 0.9992, and the experimental results are worse than the simulation. The reason for this phenomenon can be attributed to the difference between the test sample and the training sample. The training samples are generated under ideal conditions, while the test samples are recorded in the presence of noise. In addition, the incomplete alignment between the simulation data and the experimental data may also lead to errors. Adding noise to training images or using unsupervised learning algorithms to optimize the model trained on simulated data will be promising candidates for improving accuracy.

IV. Conclusion

In this paper, we have verified a promising artificial neural network-based framework to perform real-time MD for few-mode fiber through simulation and experiment. The method proposed in this work optimizes the calculation accuracy and convergence speed by combining the advantages of PCA algorithm and BP neural network. By using the proposed scheme,

the speed of complete modal demodulation can reach about 40 ms per frame. After optimizing the data set, the demodulation speed can reach about 5 ms per frame. It can also be found from the numerical example that the proposed method can still work well when the SNR level is as low as 20 dB. Additionally, the proposed scheme also has the advantages of short model training time, non-iterative, and low demand for experimental equipment. In the future, the performance of this method will be further improved by introducing far-field intensity distribution and improving BP neural network. Another promising avenue to improve performance is to apply some important methods that have not been fully utilized, such as recurrent networks (RNN), generative adversarial networks (GAN), unsupervised learning, etc., in modal demodulation tasks. In addition, to fully realize the potential of machine learning, it may be necessary to combine multiple strategies.

REFERENCES

[1] C. Schulze *et al.*, "Mode resolved bend loss in few-mode optical fibers," *Opt. Exp.*, vol. 21, no. 3, pp. 3170–3181, 2013.

[2] D. Flamm, K.-C. Hou, P. Gelszinnis, C. Schulze, S. Schröter, and M. Duparré, "Modal characterization of fiber-to-fiber coupling processes," *Opt. Lett.*, vol. 38, no. 12, pp. 2128–2130, 2013.

[3] D. Flamm *et al.*, "Fast M2 measurement for fiber beams based on modal analysis," *Appl. Opt.*, vol. 51, no. 7, pp. 987–993, 2012.

[4] T. Qiu, I. Ashry, A. Wang, and Y. Xu, "Adaptive mode control in 4-and 17-mode fibers," *IEEE Photon. Technol. Lett.*, vol. 30, no. 11, pp. 1036–1039, Jun. 2018.

[5] J. W. Nicholson, A. D. Yablon, S. Ramachandran, and S. Ghalmi, "Spatially and spectrally resolved imaging of modal content in large-mode-area fibers," *Opt. Exp.*, vol. 16, no. pp. 10 pp. 7233–7243, 2008.

[6] J. Demas and S. Ramachandran, "Sub-second mode measurement of fibers using C2 imaging," *Opt. Exp.*, vol. 22, no. 19, pp. 23043–23056, 2014.

[7] N. Andermahr, T. Theeg, and C. Fallnich, "Novel approach for polarization-sensitive measurements of transverse modes in few-mode optical fibers," *Appl. Phys. B*, vol. 91, no. 2, pp. 353–357, 2008.

[8] T. Kaiser, D. Flamm, S. Schroter, and M. Duparre´, "Complete modal decomposition for optical fibers using CGH-based correlation filters," *Opt. Exp.*, vol. 17, no. 11, pp. 9347–9356, 2009.

[9] L. Huang, J. Leng, P. Zhou, S. Guo, H. Lü, and X. Cheng, "Adaptive mode control of a few-mode fiber by real-time mode decomposition," *Opt. Exp.*, vol. 23, no. 21, pp. 28082–28090, 2015.

[10] H. Lü, P. Zhou, X. Wang, and Z. Jiang, "Fast and accurate modal decomposition of multimode fiber based on stochastic parallel gradient descent algorithm," *Appl. Opt.*, vol. 52, no. 12, pp. 2905–2908, 2013.

[11] L. Huang, S. Guo, J. Leng, H. Lü, P. Zhou, and X. Cheng, "Real-time mode decomposition for few-mode fiber based on numerical method," *Opt. Exp.*, vol. 23, no. 4, pp. 4620–4629, 2015.

[12] R. Brüning, P. Gelszinnis, C. Schulze, D. Flamm, and M. Duparré, "Comparative analysis of numerical methods for the mode analysis of laser beams," *Appl. Opt.*, vol. 52, no. 32, pp. 7769–7777, 2013.

[13] F. Stutzki *et al.*, "High-speed modal decomposition of mode instabilities in high- power fiber lasers," *Opt. Exp.*, vol. 36, no. 23, pp. 4572–4574, 2011.

[14] L. Li, J. Leng, P. Zhou, and J. Chen, "Multimode fiber modal decomposition based on hybrid genetic global optimization algorithm," *Opt. Exp.*, vol. 25, no. 17, pp. 19680–19690, 2017.

[15] E. S. Manuylovich, V. V. Dvoyrin, and S. K. Turitsyn, "Fast mode decomposition in few-mode fibers," *Nature Commun.*, vol. 11, no. 1, 2020, Art. no. 5507.

[16] W. Yan, X. Xu, and J. Wang, "Modal decomposition for few mode fibers using the fractional Fourier system," *Opt. Exp.*, vol. 27, no. 10, pp. 13871–13883, 2019.

[17] X. Wu, S. Chen, J. Huang, A. Li, R. Xiao, and X. Cui, "DDeep3M: Docker-powered deep learning for biomedical image segmentation," *J. Neurosci. Methods*, vol. 342, 2020, Art. no. 108804.

[18] X. Li, X. Fu, F. Xiong, and X. Bai, "Deep learning-based unsupervised representation clustering methodology for automatic nuclear reactor operating transient identification," *Knowl.-Based Syst.,* vol. 204, 2020, Art. no. 106178.

[19] Y. Li, Y. Xue, and L. Tian, "Deep speckle correlation: A deep learning approach toward scalable imaging through scattering media," *Optica*, vol. 5, no. 10, pp. 1181–1190, 2018.

[20] N. Borhani, E. Kakkava, C. Moser, and D. Psaltis, "Learning to see through multimode fibers," *Optica*, vol. 5, no. 8, pp. 960–966, 2018.

[21] Y. Liu, G. Li, Q. Qin, Z. Tan, M. Wang, and F. Yan, "Bending recognition based on the analysis of fiber specklegrams using deep learning," *Opt. Laser Technol.*, vol. 131, 2020, Art. no. 106424.

[22] A. Liu *et al.*, "Analyzing modal power in multi-mode waveguide via machine learning," *Opt. Exp.*, vol. 26, no. 17, pp. 22100–22109, 2018.

[23] Y. An, L. Huang, J. Li, J. Leng, L. Yang, and P. Zhou, "Learning to decompose the modes in few-mode fibers with deep convolutional neural network," *Opt. Exp.*, vol. 27, no. 7, pp. 10127–10137, 2019.

[24] H. Gao, H. Hu, Y. Zhao, and J. Li, "A real-time fiber mode demodulation method enhanced by convolution neural network," *Opt. Fiber Technol.*, vol. 50, pp. 139–144, 2019.

[25] Y. An, L. Huang, J. Li, J. Leng, L. Yang, and P. Zhou, "Deep learning-based real-time mode decomposition for multimode fibers," *IEEE J. Sel. Topics Quantum Electron.*, vol. 26, no. 4, Jul./Aug. 2020, Art. no. 4400806.

[26] Y. An *et al.*, "Numerical mode decomposition for multimode fiber: From multi-variable optimization to deep learning," *Opt. Fiber Technol.*, vol. 52, 2019, Art. no. 101960.

[27] M. Mrówczynska, J. Sztubecki, and A. Greinert, "Compression of results of geodetic displacement measurements using the PCA method and neural networks," *Measurement*, vol. 158, 2020, Art. no. 107693.

[28] Y. Song *et al.*, "Research on BP network for retrieving extinction coefficient from MIE scattering signal of lidar," *Measurement*, vol. 164, 2020, Art. no. 108028.

[29] R. Brüning, P. Gelszinnis, C. Schulze, D. Flamm, and M. Duparré, "Comparative analysis of numerical methods for the mode analysis of laser beams," *Appl. Opt.*, vol. 52, no. 32, pp. 7769–7777, 2013.

[30] J. Carpenter, B. C. Thomsen, and T. D. Wilkinson, "Degenerate mode-group division multiplexing," *J. Light Technol.*, vol. 30, no. 24, pp. 3946–3952, 2012.

[31] J. Carpenter, B. J. Eggleton, and J. Schröder, "110×110 optical mode transfer matrix inversion," *Opt. Exp.,* vol. 22, no. 1, pp. 96–101, 2014.

[32] C. Schulze *et al.*, "Mode resolved bend loss in few-mode optical fibers," *Opt. Exp.*, vol. 21, no. 3, pp. 3170–3181, 2013.

[33] L. Huang *et al.*, "Mode instability dynamics in high-power low-numerical-aperture step-index fiber amplifier," *Appl. Opt.*, vol. 56, no. 19, pp. 5412–5417, 2017.

Han Gao was born in Inner Mongolia, China, in 1995. He received the M.S. degree from Northeastern University, Shenyang, China. He is working toward the Ph.D. degree in optical engineering with Nankai University, Tianjin, China. His research interests include design and fabrication of the fiber-optic sensors, fiber modal decomposition.

Zhuo Chen received the B.S. degree from the Changchun University of Science and Technology in 2020. He is currently pursuing the M.S. degree in optical engineering with the University of Shanghai for Science and Technology. His current research interests include optical design and the manufacture of fiber lasers.

Yan-Xin Zhang received the M.E. degree from the Tianjin University of Technology, Tianjin, China. His current research interests include design and fabrication of novel fiber grating and the compound coating on fiber.

Wei-gang Zhang received the M.S. degree from Harbin Institute of Technology, Harbin, China, in 1993, and the Ph.D. degree from Nankai University, Tianjin, China, in 2002. He is a Professor with the Institute of Modern Optics, Nankai University. He has more than 200 domestic or international journal publications and more than 20 invention patents. His research interests include fiber gratings, fiber sensors, and fiber network systems. He is a recipient of three science and technology invention awards.

Haifeng Hu was born in Liaoning, China, in 1984. He received his Ph.D. degree from the Institute of Semiconductors, Chinese Academy of Sciences, China, in 2013. He is currently working with the School of Optical-Electrical and Computer Engineering at the University of Shanghai for Science and Technology. His research interests include nano-optics, plasmonics, fiber-optic sensors and their applications in biosensing. He has authored and co-authored more than 30 scientific papers, 2 patents and 5 conference presentations.

Tie-Yi Yan received the B.M. degree in clinical medicine from Harbin Medical University, Harbin, China, in 1983. She is currently a teacher and a doctor with Nankai University, Tianjin, China. Her work interests include biomedical engineering and preventive medicine.